

# Decentralized Lightweight Detection of Eclipse Attacks on Bitcoin Clients

Bithin Alangot, Daniel Reijsbergen, Sarad Venugopalan and Pawel Szalachowski  
Singapore University of Technology and Design, Singapore

**Abstract**—Clients of permissionless blockchain systems, like Bitcoin, rely on an underlying peer-to-peer network to send and receive transactions. It is critical that a client is connected to at least one honest peer, as otherwise the client can be convinced to accept a maliciously forked view of the blockchain. In such an *eclipse attack*, the client is unable to reliably distinguish the canonical view of the blockchain from the view provided by the attacker. The consequences of this can be catastrophic if the client makes business decisions based on a distorted view of the blockchain transactions.

In this paper, we investigate the design space and propose two approaches for Bitcoin clients to detect whether an eclipse attack against them is ongoing. Each approach chooses a different trade-off between average attack detection time and network load. The first scheme is based on the detection of suspicious block timestamps. The second scheme allows blockchain clients to utilize their natural connections to the Internet (i.e., standard web activity) to gossip about their blockchain views with contacted servers and their other clients. Our proposals improve upon previously proposed eclipse attack countermeasures without introducing any dedicated infrastructure or changes to the Bitcoin protocol and network, and we discuss an implementation. We demonstrate the effectiveness of the gossip-based schemes through rigorous analysis using original Internet traffic traces and real-world deployment. The results indicate that our protocol incurs a negligible overhead and detects eclipse attacks rapidly with high probability, and is well-suited for practical deployment.

**Index Terms**—Eclipse attacks, Bitcoin client, gossip protocol.

## 1. Introduction

The invention of *blockchains* as a means of providing an immutable, trustless, and de-centralized ledger promises to revolutionize monetary transfers alongside other applications. It has enabled cryptocurrencies such as Bitcoin [34] to grow without the need for a central authority, and due to its transparency has applicability in a broad range of fields including secure logging infrastructures [39], distributed timestamping [3], and micropayment channels [21]. Any user can join the Bitcoin network and view or add transactions to the distributed ledger. Since the Bitcoin network is an overlay network [42] on top of a public infrastructure (the Internet), a number of attacks on the underlying network are inherited by the Bitcoin network. For example, attacks on DNS servers arise from a lack of proper authentication, or misaligned trust between entities in the delegated DNS hierarchy. Most Bitcoin clients, including the popular *bitcoinj*, depend on

DNS seeders [1] to resolve the symbolic names of peers to their respective IP addresses. A recent survey reveal that 95% of cryptocurrencies employ DNS seeding or IP hard-coding which are censorship prone techniques [31]. If the DNS server used for name resolution by the client is compromised or malicious, then the DNS cache can be poisoned [37] to resolve the domain name to an attacker-controlled IP address. Similar attacks can be launched via insecure Internet core protocols like BGP. As discussed in the literature [28], [15], [33], [24], [26], [40], such network-level vulnerabilities make Bitcoin clients vulnerable to *eclipse attacks*, where an attacked client is connected only to attacker-controlled peers.

In this paper, we propose *two* new protocols to help Bitcoin clients detect whether they are being eclipsed. The first protocol detects eclipse attacks by using suspicious block timestamps – i.e., if the time between newly created blocks is too high, then this indicates that the network has been partitioned.

This protocol can be executed by any client in isolation, however, our analysis shows that it takes around 2-3 hours for a client to be relatively sure that it is under attack. To reduce the average attack detection times, we also propose a *ubiquitous gossip protocol* in which the client piggybacks gossip messages onto its connections to protocol-running servers. This protocol does not require any changes to Bitcoin or its peer-to-peer network. It also requires minimal support from web servers to communicate a small number of Bitcoin block headers. A server can be any host on the Internet that participates in the gossip protocol as a service to the public, and which contributes a small amount of data storage (in the order of few kilobytes) to store the gossip messages. A gossip message consists of a set of Bitcoin block headers. The server receives these gossip messages as different clients connect to it, and the server maintains the strongest view of the blockchain it has seen yet. This view is then passed to the connecting clients in exchange. The gossip protocol can function in a *passive* or *active mode*. In the passive mode, block headers are gossiped via inclusion in the HTTP(S) traffic when a client makes a standard web connection with the server. In the active mode, the client initiates connections with known protocol-running servers for the sole purpose of gossiping (to update its view of the blockchain) before it conducts a wallet balance check. We demonstrate the efficiency of our passive mode attack detection via a thorough analysis of real-world Internet traffic traces and show that, on average, the attack detection happens in less than an hour, depending on how many commonly-visited servers participate in the protocol. This time duration is typically sufficient since a block confirmation takes approximately one hour (due to the 6 block confirmation rule [11], while in reality

more confirmations may be required due to mining pool centralization).

However, in active mode the detection is almost instantaneous, although additional connections with protocol-running servers are necessary. These servers are identified through passive-mode gossiping. The requirements and attack detection time for the proposed protocols are summarized in [Table 1](#).

Various countermeasures have been proposed in the literature to detect eclipse attacks – these are discussed in [Section 3](#). Our goal is to improve on those approaches by providing a practical solution for Bitcoin clients to detect eclipse attacks. The main contributions of this paper are to *i*) propose the first (up to our best knowledge) lightweight and ubiquitous gossip protocol that can detect eclipse attacks on Bitcoin clients, *ii*) present a fully passive eclipse attack detection protocol based on “suspicious” block timestamps which does not incur additional overhead or server participation, *iii*) propose an implementation of the gossip protocols, and *iv*) thoroughly analyze the effectiveness of our protocols using real-world network traffic traces and blockchain data.

The rest of the paper is organized as follows. [Section 2](#) provides background information on Bitcoin and eclipse attacks. [Section 3](#) reviews the related work. [Section 4](#) provides an overview of the requirements and system model for the proposed the eclipse detection protocols. [Section 5](#) presents the timestamp-based protocol. [Section 6](#) presents our gossip-based protocol and analyzes the real Internet traffic trace to demonstrate its efficiency. [Section 7](#) discusses real-world deployment and privacy concerns and [Section 8](#) details the implementation and evaluation. [Section 9](#) concludes the paper.

## 2. Bitcoin and Eclipse Attacks

### 2.1. Bitcoin

Bitcoin is a distributed, peer-to-peer electronic payment system that enables Internet-based payments without going through a centralized and trusted entity like a financial institution [34]. A distributed copy of the electronic transaction ledger is stored by multiple peers of the Bitcoin network. Transactions are grouped into blocks, and the blocks are cryptographically linked forming a chain (called a blockchain). Bitcoin uses proof-of-work (PoW) for its consensus mechanism. A number of peers simultaneously attempt to solve a puzzle by finding a preimage of a cryptographic hash that satisfies the condition of the puzzle. This process is called mining. A peer that solves the puzzle broadcasts its block to other peers in the network. Peers are incentivized to create blocks as they receive a block reward and transaction fees (in Bitcoin’s native cryptocurrency called *bitcoin*). Two concurrent blocks can be mined and announced simultaneously, and in such a case peers accept the block they receive first. This process of disagreement between peers is called forking. Forking in Bitcoin is resolved by all honest peers agreeing to follow the strongest chain rule, where a chain with the most PoW aggregated is considered to be the current one. Bitcoin requires that a majority of computational power (to mine blocks) belongs to honest parties, so that they

can resolve forks in their favor and hence prevent double-spending attacks [41].

In Bitcoin, a block consists of two parts: the header [8] and the list of transactions [7]. The Bitcoin header aggregates the transactions and contains metadata – in particular, the following fields: *timestamp*, which is the (approximate) time at which the block was created, *prevHash*, which is the hash pointing to the block preceding the current block (this effectively creates a chain and provides an ordering to the blocks), and *nBits*, which encodes the block’s difficulty requirement (i.e., the amount of PoW effort required to find a solution hash to the mining puzzle). The difficulty is dynamically set every 2016 blocks in a way to adjust the average block creation time to 10 minutes. At this rate, 2016 blocks would be created in exactly 2 weeks. If it took more than 2 weeks to generate the 2016 blocks, the difficulty is reduced by adjusting the value of *nBits*. A time shorter than 2 weeks results in a difficulty increase, and a longer time in a decrease.

Peers in the Bitcoin network can, depending on their resource constraints, be categorized as mining nodes, full nodes, or simplified payment verification (SPV) nodes. Throughout the discussion, SPV nodes are also referred to as lightweight clients, light clients or clients. A mining node stores and verifies every block in the blockchain and competes to mine new blocks. A full node is similar to a mining node except that it does not work to mine blocks. An SPV client is a node that stores the block headers alone and verifies that a) each block header points to the previous block header b) and each block header was generated with the PoW required. Bitcoin aggregates transactions within blocks in a way that allows SPV clients (who only store block headers) to verify that any included transaction is part of the blockchain. To check whether a transaction has made it onto the blockchain, an SPV client makes an API call to a full node to request a proof.

### 2.2. Eclipse Attacks on Bitcoin

To handle the communication, Bitcoin introduces a peer-to-peer Internet overlay network. When a peer attempts to connect to the Bitcoin network, it first finds initial (seed) peers via a DNS lookup to pre-defined domain names. A successful DNS lookup allows the peer to contact seed peers, which in turn return lists of their known peers. The peer connects to these peers and can hence start using the protocol. The security of a Bitcoin client relies on its ability to connect to honest peers in the Bitcoin network. Being connected to an attacker-controlled Bitcoin network undermines the ability of the client to view or transact on the honest ledger, which can result in financial losses. The client may assume that it received payment in exchange for goods and services, only to realize later that the transaction was registered only on the attacker-controlled blockchain and not the canonical blockchain. Detecting such attacks is hence critical for the security of Bitcoin clients.

Unfortunately, as the Bitcoin network relies on the Internet, it inherits all its security drawbacks. Most prominently, in eclipse attacks [28], [27] an adversary manages to hijack all connections from an attacked client to other peers in the network. The client’s view of the network and information dissemination is fully under the control

		Infrastructure Support Required	Network Load	Attack Detection Time	Refer to
Timestamp		None	None	3 hours	Section 5
Gossip	passive mode active mode	Servers Servers	Natural browsing traffic Additional connections	>1 hour Immediate	Section 6

Table 1: Comparison of the proposed eclipse attack detection protocols.

of the attacker. The attacker can provide a malicious view of the Bitcoin blockchain to the client, which may include transactions of bitcoins that have already been spent on the unseen part of the blockchain’s canonical branch (this is called a *double-spend* attack). A Bitcoin lightweight client may be vulnerable to an eclipse attack through DNS cache poisoning [37] involving the name resolution of Bitcoin seeders [22], [9], or routing attacks where the Bitcoin network is partitioned [15] and the peer eclipsed.

### 3. Related work

In this section, we investigate network-level attacks on blockchain systems and their countermeasures from the existing literature. Heilman et al. [28] studied and presented the feasibility of an eclipse attack on the Bitcoin network. They showed that it is viable for a powerful adversary who controls a large number of public IPs to monopolize all peer connections to a victim Bitcoin client and consequently present a malicious Bitcoin blockchain view. The ability of an adversary to use this vulnerability to conduct selfish mining and double-spend attacks was further discussed by Gervais et al. [25] and Nayak et al. [35]. Another class of serious attacks is connected to the BGP protocol which is one of the core Internet protocols. Apostolaki et al. [15] demonstrated that the Bitcoin protocol is vulnerable to BGP routing attacks where an attacker controlling a small number of BGP prefixes can partition the Bitcoin network by announcing malicious BGP messages. To prevent such an attack, the SABRE framework was proposed [14]. It is a secure relay network which helps to protect against BGP routing attacks by enabling the Bitcoin clients to connect to relay nodes hosted at safe autonomous systems. To prevent (D)DoS attacks on relay nodes this architecture requires high-performant programmable network switches. Tran et al. demonstrated that Bitcoin clients are vulnerable to the Erebus attack [40], which is a data plane attack (in contrast to the BGP routing attack, which is a control plane attack) and hence requires no routing manipulation. This makes it much more stealthy than previous attacks. Here, an attacker who is able to control ASes that can intercept traffic to a specific set of public IPs which need not be Bitcoin client addresses can execute Erebus attacks. However, in this study (as in all studies above) a successful attacker needs to be powerful (controlling a large number of public IPs or having access to BGP routers). In contrast, Wüst and Gervais [43] as well as Marcus et al. [33] showed the feasibility of an eclipse attack on the Ethereum blockchain by exploiting vulnerabilities in its peer-to-peer protocol where an attacker needs only a small number of machines with public IPs to compromise a victim. Recently, Loe and Quaglia [31] presented a survey which shows that 95% of existing cryptocurrencies are using censorship prone technique to

bootstrapping i.e to identify peers in the network. The reason for this is attributed to code reuse of the five major cryptocurrencies. Also, the survey highlight the fact that 32% of cryptocurrencies rely on a single DNS provider for their DNS seeds leading to single point of failure. Finally, they analyze censorship resilient techniques which was found to be very inefficient with high latency overhead and none of the cryptocurrencies were able connect using this technique.

Although we are not aware of any work similar to ours, the detection and prevention of attacks on blockchain light clients is an active research topic. The popular Bitcoin light clients add hard-coded *checkpoint* block headers [5], [6] into their code bases. This helps to prevent malicious miners from reorganizing large parts of blockchain to produce a weaker view and present it to the light client. The bitcoinj light client developers have mentioned a proposal to detect eclipse attacks by analyzing the block arrival rate [1], but there is no known implementation of such a feature yet. In Section 5, we provide a detailed study on the effectiveness of such a feature in protecting light clients against eclipse attacks.

The *fraud proofs* by Mustafa et al. [13] help light clients to identify invalid blocks and reject them. The proposed data availability proofs support the light clients to gossip small chunks of information about the block for which it received a fraud proof. Therefore, the network which consists of light clients and full nodes can rebuild the complete block information to validate the proof. However, this approach requires significant modifications to the existing protocols and needs the support of a threshold number of honest light clients. The protocol is able to detect incorrect blockchain blocks, however, in contrast to our scheme fraud proofs do not detect eclipse attacks if the blocks have a valid content.

One research direction is to make light clients even lighter such that they do not have to process entire chains. Non-Interactive Proofs of Proof-of-Work (NIPoPoW) [29] and FlyClient [32] help encode blockchains such that their total PoW is expressed in a concise manner. For every chain, light clients only need to download a small proof from full nodes to make sure that their view is stronger than all known alternatives. Unfortunately, these schemes involve significant modifications to the Bitcoin protocol, e.g., Bitcoin header modification. Also, the security of NIPoPoWs is guaranteed only under certain parameter settings and in some cases it involves multiple round-trip communications between the light clients and full nodes, which increases the overhead at the light client. Although many of these issues were addressed in FlyClient, their protocol modifications form an obstacle to adaptability. Similar to the previous work, neither NIPoPoWs nor FlyClient can detect eclipse attacks by themselves – however, if deployed they could minimize the overheads introduced by our system.

Conceptually, the most related work to ours is in the context of monitoring the consistency of append-only centralized log servers as presented by Chuat et al. [19]. They propose a protocol for monitoring the consistency of certificate logs [30], where web clients exchange signed log statements via their HTTP(S) connections. This process helps to find potential inconsistencies in log statements, hence proving malice. An alternative approach for the same problem was proposed by Nordberg et al. [36], where web clients implement a feedback mechanism to inform a domain about observed log statements for the domain certificates. Due to the different setting, these schemes are not applicable in our scenario.

## 4. Solution Overview

The objective of this work is to provide lightweight methods for a Bitcoin light client to detect that it is being subjected to an eclipse attack.

Our first observation is that if a Bitcoin light client is under an eclipse attack, it is then impossible for it to detect the attack via the Bitcoin network itself (as its view is controlled by the adversary). Therefore, to facilitate detection of the attack, an external infrastructure is necessary. However, deploying a new dedicated infrastructure is a challenging task in practice. Therefore, the protocol would ideally be implemented on top of a currently existing infrastructure.

The second observation is that although the attacked light client cannot itself learn that its blockchain view is malicious, the attack is trivially detectable if any stronger concurrent view of the blockchain is available to the affected client. Permissionless blockchains, like Bitcoin, do not introduce any trusted entities that could assert which blockchain view is canonical. Instead they follow the strongest chain rule, so given two conflicting views of different strengths it is trivial to decide which is the canonical one. Therefore, the deployed detection infrastructure can be implemented as a medium for exchanging blockchain views between protocol participants. Every participant can simply compare its local view with the obtained one, detect any potential attack, and save the strongest view as the current one.

The main idea behind our gossip-based protocols is based on the observation that users of Bitcoin light clients conduct standard network connections, like web browsing, messaging, email, etc, even when their client is under an eclipse attack. Therefore, if they were to be able to exchange their blockchain views with contacted Internet servers who would store only the strongest seen view, then that could be the base for a detection system. The passive gossip scheme only uses natural traffic for attack detection. By contrast, the active gossip scheme uses natural traffic to learn of protocol-following nodes, and purposely initiates connections with a subset of them during periods of interest, i.e., when the user checks her wallet balance via the client. The timestamp-based approach uses its own principles, which will be discussed in Section 5. In the remainder of this section we present our system model and the requirements of our detection systems.

## 4.1. System Model

The main agents in our system are as follows:

- **Server (S)** is an Internet server that provides services accessible to the public and supports our protocol. Each server builds and stores its view of the blockchain from the block headers supplied to it by the clients when they establish a connection with the server. Each client sends a partial consecutive view of its block headers to the server when it connects to use its service.
- **Lightweight Client (LC)** (or just a client) is an SPV node of the Bitcoin network. Each LC obtains its view of the blockchain from the Bitcoin network that it is connected to. An LC may be under an eclipse attack, in which case it receives a malicious view of the blockchain controlled by an attacker. We assume that LCs beside Bitcoin software run other programs (e.g., a web browser) and conduct user-driven Internet connections (e.g., browsing or messaging). In this work we focus on light clients as they are the most popular and convenient way for regular users to interact with the Bitcoin network. However, our protocol can be also run by other Bitcoin clients, e.g., full nodes.
- **Attacker** is a malicious entity able to launch an eclipse attack on Bitcoin clients. The adversary may control (either directly or indirectly) enough mining power to construct an inferior branch prefixed with the canonical view of the blockchain in an attempt to masquerade as the canonical Bitcoin blockchain. The objective of the attacker is to partition the view of the Bitcoin network and provide a malicious view of the blockchain to the LC unnoticed. We assume that the adversary is not able to generate a stronger blockchain than the honest participants (or else the attacker could perform a so-called 51% attack without the need to eclipse clients).

## 4.2. Requirements

In order to realize a successful detection framework, we define the following requirements:

**Effectiveness:** participants of the detection framework should be able to detect ongoing eclipse attacks with high probability and speed. As in Bitcoin, the suggested transaction confirmation time is about one hour (i.e., six new-coming blocks after the transaction was appended), we aim for a similar time frame for attack detection.

**Low overheads:** protocol-introduced overheads should be negligible. In particular, the scheme should not require high CPU, memory, and storage utilization, and it should not introduce high bandwidth overheads or latency inflation into the existing client-server communications. The protocol should support a variety of light clients, including resource-constrained nodes like IoT devices.

**Deployability:** the protocol should be deployable without any dedicated network infrastructure. Thus, the protocol should not incur any significant investments

or setup efforts. It should use the existing infrastructure with minimal or no changes to the applications deployed on it.

**Backward compatibility:** the scheme should not require any changes to the Bitcoin protocol or its network. As witnessed from past developments and deployments, the Bitcoin community is reluctant to introduce changes to the protocol, so if such a change is required then it could undermine the deployment of the attack detection framework.

## 5. The Timestamp-Based Protocol

The first eclipse attack detection protocol that we present is fully passive and requires only the block timestamps, which are part of the block headers and therefore known to the light clients by default. Of the three presented approaches, this one has the slowest average detection time, but it is the easiest to implement as it does not depend on protocol-running servers.

During an eclipse attack, an attacker can convince a lightweight client to accept an inferior branch of the blockchain. However, to *build* such a branch the attacker will still need to control, either directly or indirectly, a considerable amount of mining power. Since Bitcoin’s mining difficulty changes infrequently, the difficulty can be assumed to remain constant for the duration of the attack. Since the attacker cannot create blocks at the same frequency as the whole network, a sudden increase in the block creation times is likely. The lightweight client *bitcoinj* has indicated that in the future, it may implement a “red alert” mode based on the block creation times [1]. To the best of our knowledge, none of the lightweight clients have implemented such a feature yet, so we present our timestamp-based protocol in this section.

### 5.1. Block Timestamp Model

Alerts in the timestamp-based approach are triggered by abnormally long block creation times. Since block creation times are random by nature, we need a probabilistic model. The time between block creations follows an exponential distribution [20], so the time needed to create  $k$  blocks in a row follows the *Erlang distribution* with shape parameter  $k$  and a mean of  $k \cdot 10$  minutes. However, day-to-day changes in the total network hash rate mean that these assumptions are not always valid. We investigate this using historical block timestamp observations and hash rate estimates that were obtained via the data API of `blockchain.com`.<sup>1</sup> In particular, we collected timestamps for the blocks between height 506000 and 560013, which were mined on Jan. 25, 2018 and Jan. 25, 2019 respectively, and which have the following hashes:  
000000000000000000000000d69a840ca2ad3560d596ccc4d2c26e7e56f4b5d18ec4e  
0000000000000000000000003cd1f6db7b2e2009e975e3baac7fc8d1c1e53f8025b8d8  
For the hash rates we collected the data underlying the hash rate estimate chart<sup>2</sup> from the 2-year period starting from 23 Jan. 2017.

As we can see in [Figure 2](#), the hash rate has changed considerably over time — it tripled between Jan. 2018

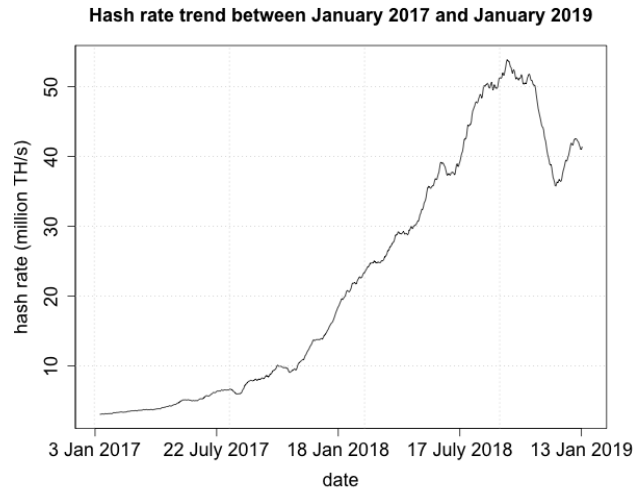


Figure 1: Bitcoin hash rate between January 2017 and January 2019, smoothed using a 14-day moving average filter (7 days on both sides).

and its peak around 18 Sept. 2018, and fell by roughly 1% per day in the 32 days from 6 Nov. to 7 Dec. The observed average block creation time between 25 Jan. 2018 and 25 Jan. 2019 was not 600 seconds, but 581, which reflects the fact for most of this one-year period, the hash rate was increasing and the difficulty therefore often too low. However, higher block creation times were observed when the hash rate was dropping. In [Figure 2](#), the observed timestamp differences are compared to an exponential distribution with a mean of 581 seconds: the fit is generally good, but more low and high extremes appear than one would expect from an exponential distribution. The assumptions underlying our calculations will be loosened to reflect this.

Since the largest observed drop in the hash rate trend since early 2017 has been 1% per day, and the Bitcoin difficulty resets every two weeks (or 16 days if we account for the dropping hash rate), we will assume that at any time the total network hash rate is at most 14-16% lower than during the last difficulty rescale. Hence, we will assume in the following that the time needed to create  $k$  blocks can be conservatively assumed to be Erlang-distributed with shape  $k$  and a mean of  $k \cdot 12$  minutes (instead of  $k \cdot 10$  minutes).

### 5.2. Alert Types

Using the probabilistic model described above, we introduce *alerts* that are triggered whenever the probability of a given sequence of block creation times is below a threshold. Different Bitcoin users require different levels of reliability, and therefore different thresholds user’s typical transactions (see also [1]). A user who cares more about fast confirmation times than security, e.g., an automated online store for video game downloads, might accept a transaction if it appears on *any* main chain block, with no confirmations needed. However, users with high security expectations, e.g., financial service providers, are more likely to use the *six-confirmations rule*, which means that they will only accept a transaction if it appears in a

1. [https://www.blockchain.com/api/blockchain\\_api](https://www.blockchain.com/api/blockchain_api)

2. <https://www.blockchain.com/charts/hash-rate>

$t$ (mins)	number of observed blocks $n$									
	0	1	2	3	4	5	6	7	12	18
20	$1.9 \cdot 10^{-1}$	$5.0 \cdot 10^{-1}$	$7.7 \cdot 10^{-1}$	$9.1 \cdot 10^{-1}$	$9.7 \cdot 10^{-1}$	$9.9 \cdot 10^{-1}$	$\approx 1$	$\approx 1$	$\approx 1$	$\approx 1$
40	$3.6 \cdot 10^{-2}$	$1.5 \cdot 10^{-1}$	$3.5 \cdot 10^{-1}$	$5.7 \cdot 10^{-1}$	$7.6 \cdot 10^{-1}$	$8.8 \cdot 10^{-1}$	$9.5 \cdot 10^{-1}$	$9.8 \cdot 10^{-1}$	$\approx 1$	$\approx 1$
60	$6.7 \cdot 10^{-3}$	$4.0 \cdot 10^{-2}$	$1.2 \cdot 10^{-1}$	$2.7 \cdot 10^{-1}$	$4.4 \cdot 10^{-1}$	$6.2 \cdot 10^{-1}$	$7.6 \cdot 10^{-1}$	$8.7 \cdot 10^{-1}$	$\approx 1$	$\approx 1$
80	$1.3 \cdot 10^{-3}$	$9.8 \cdot 10^{-3}$	$3.8 \cdot 10^{-2}$	$1.0 \cdot 10^{-1}$	$2.1 \cdot 10^{-1}$	$3.5 \cdot 10^{-1}$	$5.0 \cdot 10^{-1}$	$6.5 \cdot 10^{-1}$	$9.8 \cdot 10^{-1}$	$\approx 1$
100	$2.4 \cdot 10^{-4}$	$2.2 \cdot 10^{-3}$	$1.1 \cdot 10^{-2}$	$3.4 \cdot 10^{-2}$	$8.2 \cdot 10^{-2}$	$1.6 \cdot 10^{-1}$	$2.7 \cdot 10^{-1}$	$4.1 \cdot 10^{-1}$	$9.2 \cdot 10^{-1}$	$\approx 1$
120	$4.5 \cdot 10^{-5}$	$5.0 \cdot 10^{-4}$	$2.8 \cdot 10^{-3}$	$1.0 \cdot 10^{-2}$	$2.9 \cdot 10^{-2}$	$6.7 \cdot 10^{-2}$	$1.3 \cdot 10^{-1}$	$2.2 \cdot 10^{-1}$	$7.9 \cdot 10^{-1}$	$9.9 \cdot 10^{-1}$
140	$8.6 \cdot 10^{-6}$	$1.1 \cdot 10^{-4}$	$6.9 \cdot 10^{-4}$	$3.0 \cdot 10^{-3}$	$9.6 \cdot 10^{-3}$	$2.5 \cdot 10^{-2}$	$5.5 \cdot 10^{-2}$	$1.1 \cdot 10^{-1}$	$6.1 \cdot 10^{-1}$	$9.7 \cdot 10^{-1}$
160	$1.6 \cdot 10^{-6}$	$2.3 \cdot 10^{-5}$	$1.7 \cdot 10^{-4}$	$8.1 \cdot 10^{-4}$	$2.9 \cdot 10^{-3}$	$8.6 \cdot 10^{-3}$	$2.1 \cdot 10^{-2}$	$4.5 \cdot 10^{-2}$	$4.3 \cdot 10^{-1}$	$9.2 \cdot 10^{-1}$
180	$3.1 \cdot 10^{-7}$	$4.9 \cdot 10^{-6}$	$3.9 \cdot 10^{-5}$	$2.1 \cdot 10^{-4}$	$8.6 \cdot 10^{-4}$	$2.8 \cdot 10^{-3}$	$7.6 \cdot 10^{-3}$	$1.8 \cdot 10^{-2}$	$2.7 \cdot 10^{-1}$	$8.2 \cdot 10^{-1}$
240	$2.1 \cdot 10^{-9}$	$4.3 \cdot 10^{-8}$	$4.6 \cdot 10^{-7}$	$3.2 \cdot 10^{-6}$	$1.7 \cdot 10^{-5}$	$7.2 \cdot 10^{-5}$	$2.6 \cdot 10^{-4}$	$7.8 \cdot 10^{-4}$	$3.9 \cdot 10^{-2}$	$3.8 \cdot 10^{-1}$
300	$1.4 \cdot 10^{-11}$	$3.6 \cdot 10^{-10}$	$4.7 \cdot 10^{-9}$	$4.1 \cdot 10^{-8}$	$2.7 \cdot 10^{-7}$	$1.4 \cdot 10^{-6}$	$6.1 \cdot 10^{-6}$	$2.3 \cdot 10^{-5}$	$3.1 \cdot 10^{-3}$	$9.2 \cdot 10^{-2}$
360	$9.4 \cdot 10^{-14}$	$2.9 \cdot 10^{-12}$	$4.5 \cdot 10^{-11}$	$4.7 \cdot 10^{-10}$	$3.6 \cdot 10^{-9}$	$2.3 \cdot 10^{-8}$	$1.2 \cdot 10^{-7}$	$5.2 \cdot 10^{-7}$	$1.7 \cdot 10^{-4}$	$1.3 \cdot 10^{-2}$
480	$4.2 \cdot 10^{-18}$	$1.7 \cdot 10^{-16}$	$3.6 \cdot 10^{-15}$	$4.9 \cdot 10^{-14}$	$5.0 \cdot 10^{-13}$	$4.1 \cdot 10^{-12}$	$2.8 \cdot 10^{-11}$	$1.7 \cdot 10^{-10}$	$2.1 \cdot 10^{-7}$	$8.0 \cdot 10^{-5}$
600	$1.9 \cdot 10^{-22}$	$9.8 \cdot 10^{-21}$	$2.5 \cdot 10^{-19}$	$4.3 \cdot 10^{-18}$	$5.4 \cdot 10^{-17}$	$5.6 \cdot 10^{-16}$	$4.7 \cdot 10^{-15}$	$3.5 \cdot 10^{-14}$	$1.3 \cdot 10^{-10}$	$1.8 \cdot 10^{-7}$

Table 2: We display the probability of observing the creation of  $n$  or fewer blocks during the last  $t$  minutes, for different values of  $n$  and  $k$ . To account for natural changes in the hash rate, we assume that the time between block creations is 12 minutes (instead of 10). The coloring is as described in Section 5.2.

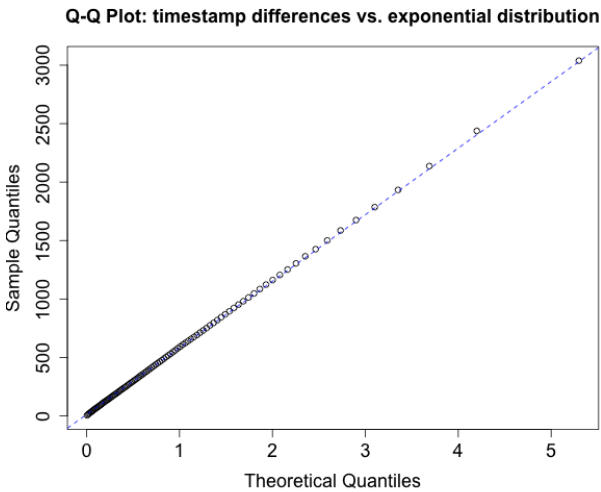


Figure 2: Comparison between the observed timestamp differences from 25 January 2018 to 25 January 2019 (with negative values removed) and the exponential distribution with the same mean as observed (581 seconds), via a Q-Q plot. Better alignment between the circles and the dashed line means a close fit. Despite the seemingly good fit, many uncharacteristically low and high values are observed, and the Kolmogorov-Smirnov test rejects the null hypothesis that the sample is drawn from the exponential distribution with a  $p$ -value of  $4.565 \cdot 10^{-7}$ . This is most likely due to considerable variations in the hash rate during this period, as observed in Figure 1. Moreover, the sample size is very large (namely  $> 50,000$ ), which means that even minor deviations from the exponential distribution will result in a low  $p$ -value.

block that has six consecutive main chain blocks built on top of it.

In Table 2, we have displayed for a range of combinations of  $t$  and  $k$ , the probability of observing  $k$  blocks during a time period of  $t$  minutes. These probabilities were computed using the statistical package R.<sup>3</sup> The probabilities have been color-coded in the following way:

3. <https://www.r-project.org/>

a cell in Table 2 is colored yellow  $\square$ , orange  $\square$ , or red  $\square$  if the corresponding probability is lower than  $10^{-2}$ ,  $10^{-4}$ , or  $10^{-6}$  respectively — the cell is colored green  $\square$  if it neither. To compare this to certainty thresholds that are common in the scientific literature: for hypothesis testing in social science and clinical trials and threshold of 5%, i.e.,  $5 \cdot 10^{-2}$  is used, whereas the ‘five sigma’ rule used to mark a discovery in physics correspond to  $2.87 \cdot 10^{-7}$ . Although the choice of thresholds for the alert types is necessarily subjective, the yellow and red flag thresholds were chosen to be roughly between these values. Yellow flags might occur relatively even under normal circumstances: since 144 blocks are mined per day, an average 1.44 blocks per day will have a creation time that is in the top 1%. If the number of false alarms is too high, then this by itself may be inconvenient to the user — in any case, the exact alert level at which a user is comfortable accepting a transaction depends on her preferences.

In practice, we recommend the following scheme. We aim to detect two types of eclipse attacks: 1) an attacker without any significant mining power on her chain performing a DoS attack, and 2) an attacker with significant mining power who aims to double-spend. Regarding 1), the lightweight client tracks how much time has passed since the creation time (indicated by the timestamp) of the last block. If this is longer than approximately 55, 110, or 165 minutes, then this throws a yellow, orange, or red flag, respectively (these values are derived directly from the exponential distribution). For attack 2), we keep track of the creation times of the last  $k + 1$  blocks, where  $k$  is the number of confirmations. If  $k = 6$ , then this is longer than approximately 190, 275, or 350 minutes, then this throws a yellow, orange, or red flag, respectively (these values are derived from the Erlang distribution). To summarize, although one would normally expect 7 blocks to be mined after 70 minutes, one should get suspicious if it took three hours, and if it took six hours one can say with near-certainty that an attack is taking place.

**Timestamp Reliability.** We have so far assumed that the timestamps are reliable: our analysis shows that under normal circumstances this is a reasonable assumption,

even though small deviations are tolerated by miners and lightweight clients [38]. In 0.5% of all blocks observed in the study period, the timestamp was *lower* than the timestamp of the previous block, although these differences were often less than 30 seconds. These observations were discarded to create Figure 2. Deviations may occur because even honest miners have considerable freedom when choosing the block timestamps. For example, the miner could choose to fix the timestamp when she starts to mine a new block, or update the timestamp continuously while mining. If different miners follow different rules, then this may lead to deviations from the exponential distribution. Furthermore, network latency adds a period of time with an unclear probability distribution between the creation of a block and the start of the mining process for the next block. Still, our analysis of real block timestamps suggests that these effects are negligible compared to the roughly 10 minutes on average between block arrivals, and that they do not have a major effect on the shape of the tail (i.e., the likelihood that very large values occur).

During an attack, the attacker is also free to set the timestamps at will. This has no effect if the attacker is performing a DoS attack, because in that case the attacker is not mining blocks. However, if she is trying to double-spend, then she can choose the timestamps such that the blocks appear to have been mined earlier. To ameliorate this, the client can also consider the times at which the blocks are first observed *by the client* instead of the timestamps in the block headers. Let  $\Delta$  denote the difference between the arrival time of the last block and the client’s current system clock. The client can then add  $\Delta$  to the total time for the seven blocks – after all, this is a lower bound on the last block’s contribution to the total. Again, there are some concerns regarding the effect of the network latency on the probability distribution of the times between block arrivals. We leave the evaluation of whether the exponential distribution is still a good fit in this setting as future work.

### 5.3. Attack Analysis

In Table 3, we have displayed for several values of  $\alpha$  the probability that an  $\alpha$ -strong is able to create 7 blocks without triggering an alert, for each of the four alert types. We assume that the attacker controls at most 50% of the mining power, as otherwise it would be easier to perform a 51% attack on the whole network without eclipsing specific clients. We see that even for a 20%-strong attacker, the probability of creating 7 blocks without of triggering a yellow alert is less than 1.7%. For a 5%-strong attacker, the probability of not triggering a red alert is already less than 0.01%. This means that an attacker will need considerable mining power to perform double-spend attacks without the risk of causing alarm, even when simultaneously performing an eclipse attack.

## 6. Gossip-Based Protocol

In this section, Section 6.1 discuss the overview of the gossip-based protocol, Section 6.2 give protocol description of passive-based gossiping approach and Section 6.3 provides a detailed analysis of its effectiveness. Last, Section 6.4 shortly discuss an active-based gossiping

$\alpha$	yellow <span style="color: yellow;">■</span>	orange <span style="color: orange;">■</span>	red <span style="color: red;">■</span>
0.05	$2.05 \cdot 10^{-6}$	$2.72 \cdot 10^{-5}$	$1.40 \cdot 10^{-4}$
0.08	$5.78 \cdot 10^{-5}$	$6.40 \cdot 10^{-4}$	$2.82 \cdot 10^{-3}$
0.125	$1.10 \cdot 10^{-3}$	$9.34 \cdot 10^{-3}$	$3.28 \cdot 10^{-2}$
0.2	$1.68 \cdot 10^{-2}$	$9.44 \cdot 10^{-2}$	$2.33 \cdot 10^{-1}$
0.3	$1.13 \cdot 10^{-1}$	$3.85 \cdot 10^{-1}$	$6.46 \cdot 10^{-1}$
0.5	$5.47 \cdot 10^{-1}$	$8.85 \cdot 10^{-1}$	$9.77 \cdot 10^{-1}$

Table 3: We display the probability that an  $\alpha$ -strong attacker is able to create 7 blocks within a period that is short enough to not trigger an alert, for each of the 3 alert types.

approach which helps to further improve detection time. The notation used to describe our gossip-based protocol is presented in Table 4.

Notation	Description
$S$	a server participating in the protocol
$LC$	a (light) client participating in the protocol
$V_{LC}$	a blockchain view of $LC$
$V_S$	a blockchain view of $S$
$HDR_{S \rightarrow LC}$	a set of block headers send from $S$ to $LC$
$HDR_{LC \rightarrow S}$	a set of block headers send from $LC$ to $S$

Table 4: Summary of the used notations.

### 6.1. Protocol Overview

Bitcoin is a trustless, decentralized network and our approach for detecting eclipse attacks follows these core principles. The proposed protocol does not implicitly need to trust any one server in the gossip network. Rather, it assumes that if a client can connect to at least one server with a legitimate view of the blockchain, then a potential eclipse attack can be detected. In our approach client-server connections are driven by the user’s natural Internet traffic. For every such connection, a client piggybacks its blockchain view to the server, which in turn returns its strongest view. Afterwards, the communicating parties can update their views according to the strongest chain rule. In such an approach, servers are passive and not connected to the Bitcoin network, but they maintain their strongest blockchain views based on the input from clients.

To illustrate the process better, we depict the main elements and intuitions behind our framework in Figure 3. Let us consider the selected case where there are three servers and three clients supporting our scheme. Clients  $LC_1$  and  $LC_2$  are connected to the genuine Bitcoin network  $BN_1$  with the  $BC_1$  blockchain view (i.e., headers), while the client  $LC_3$  is under an eclipse attack and connected to the malicious  $BN_2$  with the view  $BC_2$ . The agents communicate in the following sequence:

- 1) The clients  $LC_1$  and  $LC_2$  holding genuine blockchain views contact the server  $S_1$ , which after their connections validates and accepts the received (authentic) view.
- 2)  $LC_3$  is eclipsed and connected to a malicious Bitcoin network partition  $BN_2$ , and while connecting to the server  $S_3$  (without any current view), the malicious view is accepted by the server.
- 3) Afterwards, the attacked client  $LC_3$  connects to the server  $S_2$ . The server and client exchange their blockchain views.

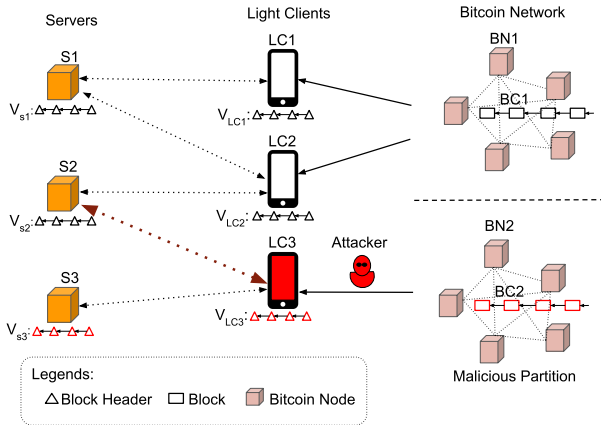


Figure 3: Proposed eclipse attack detection model comprising of servers, light clients, the Bitcoin network, and the attacker. Blocks/headers that are colored red were created by the attacker.

- 4) The server  $S_2$  stores the received headers from the client  $LC_3$ . It validates the view received from  $LC_3$  and picks the chain that corresponds to the strongest view (which is expected to be part of the canonical blockchain). The server sends its (strongest) view to the client.
- 5)  $LC_3$  is now able to detect that it is under an eclipse attack just by concluding that there exists a stronger blockchain than the one obtained from the malicious partition.

We emphasize that in *passive mode* gossiping, the detection process is driven by natural Internet traffic as participating servers are assumed to already exist (e.g., running web services), and the protocol messages are piggybacked on the standard client-server connections. In the case of *active mode* gossiping, we assume that clients make explicit connections with known servers to compare their view of the blockchain with that of the servers before when they check their wallet.

## 6.2. The Passive Gossip-Based Protocol

In Section 5, we saw that based on timestamps alone, a user can at best get suspicious after an hour and be almost certain of an attack after roughly three hours. If the attacker controls some mining power on her branch, then attack detection is even slower. In this section, we propose a gossip-based protocol to detect eclipse attacks more rapidly. It is described as a series of interactions between the server, lightweight client, and the Bitcoin network. The client-server communication is part of the natural client's traffic whereas the client-Bitcoin network communication is on demand, like today. The main goal of the client-server communication is to provide a client, via a server, with the strongest view of the chain the server has seen. To achieve this, a lightweight client forwards to a contacted server headers obtained from the Bitcoin network. When a server communicates with multiple clients, the server stores the strongest view of the chain it has received and serves this view to connecting clients. As a result, a client viewing a malicious partition of the Bitcoin network is able to fetch the strongest chain

seen by the server and compare with its own. When the server has a stronger view of the chain, the client can conclude that it is under an eclipse attack. In addition to detecting eclipse attacks, we propose a Bitcoin header size optimization to reduce communication overheads. We choose the headers of HTTP(S) request/response messages as a communication medium of our gossip layer due to the ubiquitous nature of HTTP(S). Furthermore, if HTTPS is used then the message headers are encrypted, which means that a man-in-the-middle attacker cannot distinguish these messages from normal traffic. We discuss the implications of our choice in Section 6.2.5. We focus on the passive version of the protocol in this section, and shortly discuss the active version in Section 6.4.

**Storage Requirement.** The storage on the client and the server is a fixed-length sequence of Bitcoin headers, referred to as a queue or window. New headers enter at the *tail* of the queue and old headers exit at the *head*. The client and server windows are of equal size. As we explain later, the maximum storage requirement on a client/server is 2016 times 80 bytes, i.e., around 160 kB and we can also compress it as mention in Section 6.2.4 to reduce storage requirement by half. Here, 2016 corresponds to the average number of Bitcoin blocks generated in two weeks and 80 bytes is the Bitcoin header size.

**Network Interactions.** The main agents of our protocol are the server(s), client(s), and the Bitcoin network. A client may have newly joined, or been offline for a period of time. The first step for the client is to get its headers up-to-date from the Bitcoin network. It may, however, get updated with malicious headers when it is under an eclipse attack. The second step is the exchange of headers between the client and a protocol-running server via HTTP(S) messages. However, a server that starts to deploy our protocol may have an empty window and no headers to send. If this is the case, it accepts the headers provided by the client and returns an empty (NULL) window to the client. The message exchange that follows is discussed in Section 6.2.1. The third step is to match the views on the client and server. This is discussed in Section 6.2.2. The final step is to find the strongest chain, as we discuss in Section 6.2.3. Section 6.2.4 presents an optimization technique for the block headers to save both storage and bandwidth. Section 6.2.5 discusses the choice of layer used for message exchange.

### 6.2.1. Message Exchange Between Client and Server.

In the following, we assume that a client has a copy of the headers from the Bitcoin network, but is unable to ascertain whether they belong to an inferior chain created by an attacker. Hence, the client wishes to connect to a server or group of servers and confirm the veracity of the headers it received via its natural HTTP(s) connections. The message exchange between the client and a server begins with a service request from the client.

Figure 4 outlines the message exchange between the client and the server. We note that the header index of the genesis block is 0 and we define *last* as the index of the latest header. This would ensure that both chains are compared over the same index range avoiding offset calculation mistakes (please note that Bitcoin headers do



not contain any sequence numbers). Let  $range = [beg, end]$  be the sequence of blocks between a given beginning and ending index, respectively. The messages exchanged are *i*) a request for headers in a range or *ii*) a set of headers.

The gossip message created by the client is a *range* of headers and is communicated to the server which handles the gossip message received. The set of requested headers ( $HDR_{S \rightarrow LC}$ ) and a new *range* are sent to the client, who responds to the server with the requested headers ( $HDR_{LC \rightarrow S}$ ). The client and the server have now completed their exchange of headers.

---

**Algorithm 1:** Find *strongest* chain given 2 views

---

```

input :  $V_{LC}, V_S; V_{LC} \neq V_S$ 
output: strongestChain

1 function findStrongestChain ( $V_{LC}, V_S$ )
2   strongestChain  $\leftarrow \{\}$ ;
3   sWeight  $\leftarrow 0$ , cWeight  $\leftarrow 0$ ;
4   foreach  $b \in V_{LC}$  do
5     | targetHash  $\leftarrow$  find_target( $b$ );
6     | cWeight  $\leftarrow$  cWeight + targetHash;
7   end
8   foreach  $b \in V_S$  do
9     | targetHash  $\leftarrow$  find_target( $b$ );
10    | sWeight  $\leftarrow$  sWeight + targetHash;
11  end
12  if cWeight > sWeight then
13    | strongestChain  $\leftarrow V_S$ ;
14  end
15  else if cWeight < sWeight then
16    | strongestChain  $\leftarrow V_{LC}$ ;
17  end
18  return strongestChain;

```

---

**6.2.2. View Matching.** Once the messages have been exchanged, the next step is to compare them. However, it needs to be ensured that comparisons are over

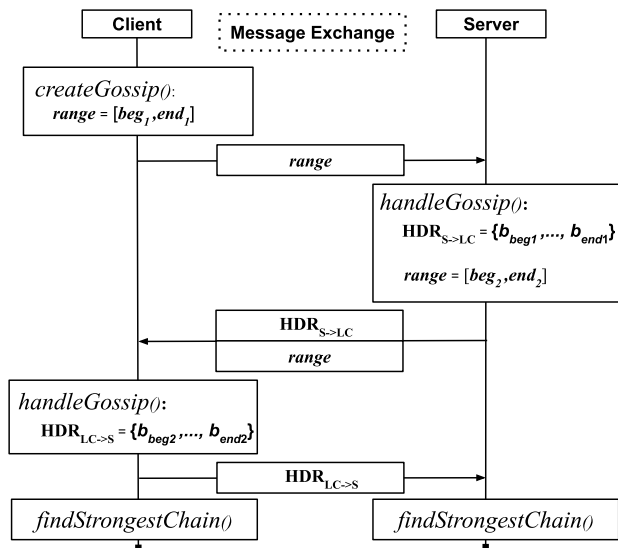


Figure 4: Header exchange between client and server.

the same range of headers. To achieve this goal, we formalize the view on the server and the client. The server view is its window of the latest headers:  $V_S = \{b_{n+1}, \dots, b_{n+k}\}$ . The client view is  $V_{LC} = \{\hat{b}_{n+1}, \dots, \hat{b}_{n+k}\}$ . Note that the server and client exclude headers received from their most recent message exchange. Hence, we have,  $V_S \leftarrow V_S \setminus b; \{b : b \in HDR_{LC \rightarrow S}, b \notin V_S\}$  and  $V_{LC} \leftarrow V_{LC} \setminus b; \{b : b \in HDR_{S \rightarrow LC}, b \notin V_{LC}\}$ . The excluded headers from their current view are added after the strongest chain is computed (see Section 6.2.3). This ensures that comparisons are not made on the same copy of headers exchanged from one side to the other.

When no forks are detected, the server and the client are viewing the same set of headers and  $b = \hat{b}$ . When a fork is detected at  $b^* \in V_S, V_{LC}$ ; the subsequent  $b \neq \hat{b}$ . Here, the server and client are viewing the same set of header up to  $b^*$ , and the subsequent views diverge. The fork is resolved by following the Bitcoin's *strongest* chain applied to views. All message exchanges in a window of size  $k$ , are bounded to  $2*k$  header transfers, for one round of client-server communication. The ability of the client to detect and resolve a fork is limited to forks occurring within the window. For instance, a window size of  $k = 2016$  corresponds to roughly 2 weeks (for an average inter-block time of 10 minutes) and a client who is offline for this period is still able to detect a fork. The size of the window is a system parameter and may be increased to support a longer detection period.

**6.2.3. Finding the Strongest Chain.** Once the views are matched, the client and server are ready to find the *strongest* chain. By the nature of the message exchange, clients and servers may see different views of the chain over a period of time (within the same range). When presented with two views, they pick the stronger chain as specified by the Bitcoin protocol (note that any stronger chain presented can convince an attacked client that she is under the attack). This process is repeated for every round of a message exchange and the full algorithm is described in Algorithm 1, taking the views  $V_S$  and  $V_{LC}$  as input and outputting the *strongest* chain. Lines 4-7 and 8-11 calculate the cumulative sum of the proof-of-work of the headers in  $V_{LC}$  and  $V_S$  respectively (which is derived from  $nBits$  [10] for each header). Lines 12-17 compare the cumulative sum to decide on the *strongest* chain. Recall that for a smaller target hash, a higher hash rate is required to solve a proof-of-work puzzle. As a result, the smaller cumulative sum determines which view is stronger. Once the strongest chain is determined at the server, all  $\{b : b \in HDR_{LC \rightarrow S}, b \notin V_S\}$  that can form a valid chain are added to  $V_S$ . Similarly, at the client, all valid  $\{b : b \in HDR_{S \rightarrow LC}, b \notin V_{LC}\}$  are added to  $V_{LC}$ . Note that the window is implemented as a fixed-length FIFO queue. The last step of extending the view is to prepare the protocol for the next round of communication. Headers are not checked if they are part of the strongest chain seen yet.

**6.2.4. Header Size Reduction.** As our protocol requires that blockchain fragments (i.e., consecutive block headers) are sent between clients and servers, we propose a way of minimizing this overhead. The main intuition behind our modification is that the *prevHash* field of

the Bitcoin header can be computed from the previous header. Therefore, for a subchain consisting of consecutive block headers, only the first header has to include its *prevHash*, whereas every subsequent header can compute it recursively. Another observation is that some header fields have either constant or infrequently changing values.

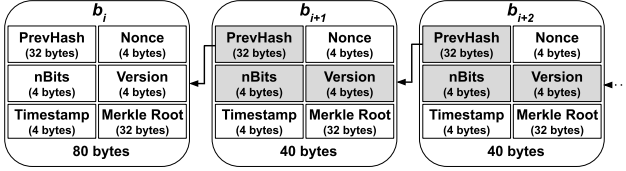


Figure 5: Header size reduced by removing *version*, *nBits* and *prevHash* fields.

In Figure 5, we present a header list where the full header is only stored in  $b_i$ , whereas  $b_{i+1}$  and  $b_{i+2}$  have their highlighted fields removed. While each Bitcoin header is 80 bytes in size, it is unnecessary to store all fields as *nBits* is fixed for 2015 consecutive blocks, *version* changes infrequently, and *prevHash* can be recalculated as described above. Hence, in our protocol we remove *nBits* (we send it only for difficulty changes – every 2016 blocks), *version* (we send it only for version changes), and *prevHash* fields from most headers that are part of the message exchange. These changes help us to reduce the size of a typical header from 80 to only 40 bytes.

**6.2.5. Gossip Layer.** As mentioned before, we have implemented our protocol by appending the block headers to the header of an HTTP request-response. This facilitates the easier deployment of our protocol as no higher-level protocol modifications are required. Also appending additional data into the HTTP header does not break applications not supporting our protocol since server drops any unnecessary data in the header without affecting the protocol. Though HTTP protocol specification does not specify any limit on the amount of data that can be sent in a HTTP headers, web servers usually restrict the size to 4k-64k. However, this limit is configurable and can be set according to the requirement of our protocol. Although selecting HTTP as gossiping medium make our protocol application specific means exclude non-HTTP(S) traffic that can also be leveraged to gossip, we have found that in practice, HTTP(S) dominates Internet traffic. In fact, non-HTTP(S) traffic only accounts for 12% of Internet traffic in our dataset. This is discussed in more detail in Section 6.3. We note that different choices for the gossip layer could be made, e.g., the HTTP(S) body could be modified instead, or TCP headers could be used to capture a broader category of traffic. However, TCP header modification could have unforeseen effects on middleware that would undo any advantages. For completeness, we present implementations of gossip medium with TCP in Section A to make our scheme application-agnostic and HTTP body in Section B.

### 6.3. Analysis of the Passive Gossip Protocol

In this section, we analyze real Internet traffic trace to demonstrate that our approach of *passive mode* gossiping is practical and efficient compared to the timestamp-based

protocol of Section 5. In fact, a user may be able to detect with certainty that she is under attack in roughly one hour compared to 3 hours previously. We first discuss the data in Section 6.3.1. We discuss our exact evaluation metrics — coverage of client IPs, speed of attack detection, and server freshness — in Section 6.3.2. We evaluate these metrics using the data in Section 6.3.3.

**6.3.1. Description of Data.** To understand the Internet access pattern of users we analyze the traffic log from a university firewall<sup>4</sup>. The users authenticate to the firewall before they access the Internet. This allows us to obtain access details of their devices to public IP addresses from the firewall traffic log. As the user devices are assigned IPs through DHCP, we identify users by their user name rather than their DHCP-assigned IP address<sup>5</sup>. In some cases, users access public servers within the university network through a private IP, hence we also include those IP addresses to analyse our protocol. In order to include only traffic in which we can gossip (via HTTP(S) message bodies), we make use of the *port* field in the traffic log. We also consider connections which were blocked by the firewall, since we assume that these connections would have succeeded outside the university.

In total, we collected 72 hours of continuous firewall traffic log. This included 229,374 unique client IPs (assigned using DHCP) and 269,069 accessed server IPs. However, these client IPs were mapped to 2511 users and we selected 43277 server IPs that were active in at least 4 out of 12 epochs (the total 72-hour time period was divided into 12 epochs). In order to understand the user activity, every 24 hours (representing a day) was divided into 15-minute slots. The average number of connections for each slot across the 72 hrs of traffic log is represented in Figure 6. We can see that user activity is high during certain time intervals (active periods) and less so during other time intervals (inactive periods) — we assume that many users are sleeping during the inactive period. Later, we explain how these inactive periods influence our results.

**Ethical Consideration.** The traffic log was provided to carry out research without breaching any user privacy policy. We obtained the following details: timestamp, server IP, client IP, action and a unique string representing the user’s ID. No other details regarding the users were used for analysis. We do not publish the dataset with this paper, and as such its use constitutes *minimal risk* to the users.

**6.3.2. Methodology.** Given the full dataset, let  $\mathcal{U}$  be the full set of users, and  $\mathcal{S}$  the full set of server IPs observed. Furthermore, let  $t_0$  and  $t_{\max}$  be the times of the first and last connections respectively, and  $\mathcal{T} = [t_0, t_{\max}]$ . We can then extract from the dataset the full set  $\mathcal{C}$  of connections, where each connection  $c \in \mathcal{C}$  is a tuple  $(u_c, s_c, t_c)$ , such that

4. We do not disclose the university name to comply with the double-blind review process.

5. In accessible traffic datasets, users are not identifiable. Hence, it is necessary to assume the user:IP mapping. Our dataset allows to associate users with connections, to improve the accuracy of our study and to make it realistic.

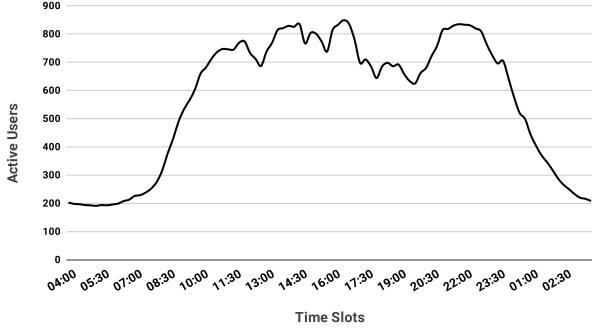


Figure 6: The traffic logs of 24hrs are divided into 15 minutes time-slots and average of total traffic in each slot across the 72hrs traffic log is represented in the graph.

- $u_c \in \mathcal{U}$  is the ID of the user who initiates the connection,
- $s_c \in \mathcal{S}$  is the IP address of the server, and
- $t_c \in \mathcal{T}$  is the initiation time of the connection.

We then use  $\mathcal{C}$  to define the following metrics for the performance of the gossip-based approach:

**Coverage:** given a set  $S \subset \mathcal{S}$  of servers, we define its coverage as the fraction of unique users that at some point connect to a server in  $S$ . This can be formally expressed as

$$\text{Coverage}(S) = \frac{|\{u \in \mathcal{U} : \exists c \in \mathcal{C} \text{ such that } s_u \in S\}|}{|\mathcal{U}|},$$

where  $|A|$  denotes the number of elements in set  $A$ .

**Attack Detection Speed:** given a user  $u \in \mathcal{U}$  and a set  $S \subset \mathcal{S}$  of servers, we define the *attack detection speed* as the time until the next connection from  $u$  to a server in  $S$ . To make this formal, we first define  $C_{u,S}$  as the set of all connections to  $S$  initiated by  $u$ , i.e.,

$$C_{u,S} = \{c \in \mathcal{C} : u_c = u \text{ and } s_c \in S\}.$$

For any  $t \in \mathcal{T}$ , let  $T_{u,S}(t)$  be the set of all time points *after*  $t$  at which  $u$  connects to a server in  $S$ . That is,

$$T_{u,S}(t) = \{t' \in \mathcal{T} : \exists c \in C_{u,S} \text{ such that } t_u = t' \text{ and } t_u > t\}.$$

We then define  $\delta_{u,S}(t)$  as the time from  $t \in \mathcal{T}$  until  $u$ 's next connection to a server in  $S$  (or until  $t_{\max}$ ). That is,

$$\delta_{u,S}(t) = \begin{cases} \min(T_{u,S}(t)) - t & \text{if } T_{u,S}(t) \neq \emptyset, \\ t_{\max} - t & \text{otherwise.} \end{cases}$$

(Note that  $T_{u,S}(t) \neq \emptyset$  only for  $t$  after the time of the last connection, at which point we consider a connection to occur exactly at the end of the observation period.) We will assume that attacks occur at a time that is drawn uniformly from  $\mathcal{T}$ . The Average Attack Detection Time (AADT) for  $u$  to  $S$  is then given as follows:

$$\text{AADT}(u,S) = \frac{1}{t_{\max} - t_0} \int_{\mathcal{T}} \delta_{u,S}(t) dt \quad (1)$$

The reasoning behind (1) is as follows. Let the time at which the attack occurs be given by the random variable

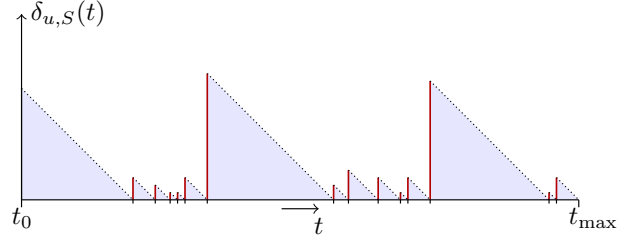


Figure 7: Graphical illustration of the average attack detection times given a user  $u$  and a set of servers  $S$ . Connections from  $u$  to a server in  $S$  occur at the time points indicated by the vertical red bars. The dotted lines represent  $\delta_{u,S}(t)$  — the time of the next connection after  $t$ .

$T^*$ , and its probability density function by  $f_{T^*}(t) : \mathcal{T} \rightarrow [0, \infty)$ . It then holds<sup>6</sup> that

$$\mathbb{E}(\delta_{u,S}(T^*)) = \int_{\mathcal{T}} \delta_{u,S}(t) f_{T^*}(t) dt, \quad (2)$$

where  $\mathbb{E}$  denotes the expected value of a random variable. Substituting  $\frac{1}{t_{\max} - t_0}$  for  $f_{T^*}(t)$  (which follows from the uniform distribution of the attack times) into (2) then leads to (1).

A graphical representation of the AADT is given in Figure 7. In this example, the connections occur at the locations of the vertical red bars, and the height of the red bar indicates the amount of time until the next connection. The function  $\delta_{u,S}$  is represented by the dotted lines, and the area of the blue triangles represents the integral in Equation 1.

**Server Freshness:** given a server  $s \in \mathcal{S}$  and a set  $U \subset \mathcal{U}$  of users, we define the *freshness* as the time since the previous connection from a user in  $U$  to  $s$ . It can be defined in a similar way as the attack detection time. That is, let  $T'_{s,U}(t)$  be defined as the set of all time points *before*  $t$  at which a user in  $U$  connects to  $s$ . Then  $\eta_{s,U}(t)$  is the amount of time since the last connection by a user in  $U$  to  $s$ , defined as follows:

$$\eta_{s,U}(t) = \begin{cases} t - \max(T'_{s,U}(t)) & \text{if } T'_{s,U}(t) \neq \emptyset, \\ t - t_{\min} & \text{otherwise.} \end{cases}$$

The average server freshness can then be defined as follows:

$$\text{Freshness}(s,U) = \frac{1}{t_{\max} - t_0} \int_{\mathcal{T}} \eta_{s,U}(t) dt \quad (3)$$

A graphical representation of  $\eta_{s,U}(t)$  would look similar to Figure 7, but with the triangles flipped horizontally.

**Active/Inactive Periods.** As can be seen from the Figure 7, long periods of inactivity — represented by the three large triangles — have a considerable impact on the AADT. One typical period of inactivity is the period between 2:00AM and 7:30AM (see also Figure 6), although longer periods (where users are offline for at least a day) are also regularly observed in the dataset. To mitigate this, we propose the following feature: if a user's view has

6. See, e.g., [https://en.wikipedia.org/wiki/law\\_of\\_the\\_unconscious\\_statistician](https://en.wikipedia.org/wiki/law_of_the_unconscious_statistician)

not been updated for over *eight hours*, then an alert is triggered. This is incorporated in the computation of the AADT by removing all time periods that correspond to at least eight hours of inactivity.

**Stratified Sampling.** In the following, we will also divide the servers into several *tiers*: tier 1 contains servers with 1601-3200 unique users access, tier 2 those with 801-1600 access, up to tier 6 with less than 100 access. If we choose a random sample  $S$  of servers, the tiers that the chosen servers belong have a strong impact on our results — e.g., if all the servers are drawn from tiers 5-6 then the coverage will be poor, whereas even one server from tier 1 would improve the results dramatically. Hence, in [Section 6.3.3](#) we will use a stratified sampling method that ensures that our sample contains servers from each of tiers 1-4.

**6.3.3. Results.** The tables for the empirical results for the coverage, AADT, and average server freshness in [Tables Table 5](#), [Table 6](#), and [Table 7](#) respectively. In all of our experiments, we group the servers in our dataset into five groups such that servers in each group either belong to the same organization or within a specific IP range. This is only a way of selecting the servers to run our protocol to show the effectiveness, there is no strict rule on which servers can adopt our protocol. Any public server offering a service to the users can help with gossiping, more the number of servers the faster the attack detection.

Groups	tier 1		tiers 1-4	
	$n_s$	Coverage	$n_s$	Coverage
Group 1	107	0.996	731	0.996
Group 2	23	0.99	399	0.991
Group 3	32	0.981	1642	0.99
Group 4	9	0.982	42	0.982
Group 5	10	0.93	64	0.953

Table 5: Results for the coverage (in hours) for the servers of different five different groups.

In [Table 5](#), we display the coverage results for the five groups.

Groups	tier 1		tiers 1-4	
	$n_s$	AADT	$n_s$	AADT
Group 1	107	0.793	731	0.788
Group 2	23	0.862	399	0.843
Group 3	32	1.011	1642	0.868
Group 4	9	0.944	42	0.929
Group 5	10	1.122	64	1.13

Table 6: Results for the AADT (in hours) for the servers to five different groups.

In [Table 6](#), we display the results for the AADT during the active periods, averaged across all 2511 users. We see that in each case, the average time to detect is around one hour. This can be achieved by just a handful of popular servers, e.g., Group 4’s 9 or Group 5’s 10 most popular servers. In most cases, the lower-tier servers do not contribute much to performance — the exception is Group 3, which has a very large number of lower-tier servers, which is probably due the servers being part of a large cloud service provider.

$p_u$	$n_u$	tier 1	tiers 1-4
0.01	25	$0.801 \pm 0.0619$	$1.716 \pm 0.0566$
0.03	75	$0.492 \pm 0.0478$	$1.553 \pm 0.0426$
0.1	251	$0.264 \pm 0.017$	$1.137 \pm 0.0282$
0.3	753	$0.155 \pm 0.0045$	$0.863 \pm 0.014$
1.0	2511	$0.109 \pm 0.0$	$0.591 \pm 0.0$

Table 7: 95%-confidence intervals for the average server freshness (in hours) for different user adoption percentages  $p_u$ . We use random sampling with 8 experiments.

In [Table 7](#), we have displayed the results for the server freshness. We considered different user adoption rates, ranging from 1% to 100%. For each of the given percentages, we draw a random sample among the users, and repeat this experiment 8 times to create 95% confidence interval for each entry. We see that even 25 active users can maintain an average server freshness of below one hour. Note that by a 100% adoption rate we just refer to the users in this dataset, and that for a real highest-tier Group 4 & 5 (servers in this group mainly offers social networking services.) servers, 2500 active lightweight client users may not be unrealistic.

## 6.4. The Active Gossip-Based Protocol

We have seen that the passive mode gossip protocol reduces average attack times from three hours to around one hour. To improve this even further, the *active mode* gossip protocol initiates connections to known protocol-running servers before certain events. One typical event is a user checking her wallet balance using the client — since, she is at the risk of making erroneous decisions if her client is being eclipsed as part of a double-spend attack. To obtain knowledge of protocol-running servers, the client builds a list of servers while it does passive gossiping. That is, if the server is able to interpret the additional *range* field in the HTTP(S) request and send back the requested block headers within that range in the corresponding HTTP(S) response, then client in addition to running our protocol (passive) add the IP address of the server to the list, if previously unknown. After a triggering event, a random selection of the known servers are polled from this list — the size of this selection depends on the client, as more servers means a better chance of detection, but more additional traffic. If an up-to-date server is contacted, then eclipse attack detection is almost instantaneous during periods of interest.

In some cases, e.g., if the server is hosting a website associated with a block explorer (e.g., [blockchain.com](#)) or a cryptocurrency exchange (e.g., [binance.com](#)), then the company that runs the server is likely to run its own full node anyway, which makes a link even more natural.

## 7. Discussion

In this section, we discuss the real-world implementation of our approach. As the deployment of the timestamp-based approach is straightforward (see [Section 5](#)), we limit this discussion to the gossip protocol.

## 7.1. Real-World Deployment

In contrast to competing techniques [14], one of our design goals is to not require any additional infrastructure. The gossip protocol works in a distributed way, as anyone can join the network by launching a supporting server. The dataset used for the analysis mainly consist of traffic towards web service providers whom we assumed to be willing to deploy our gossip protocol on their servers. We then evaluated the time required for a typical Internet user to detect an eclipse attack (analyzed based on our network traffic data). We selected the most popular (by user interactions) Internet servers to model the typical pattern of connections between a user and a service. However, in practice, it is difficult to determine which servers or organizations would be willing to support the protocol, and we see this as a limitation of our analysis.

Finally, we note that although we considered adoption by specific set of servers categorized into five groups for our analysis, we do not introduce any centralization factors with it since any number of different entities can run our protocol simultaneously and independently.

## 7.2. Privacy

Our protocol is privacy-friendly since lightweight clients gossip only block headers and do not execute any payment verification with the gossip servers. Hence, neither Bitcoin wallet addresses nor transaction information is conveyed to the server. Although lightweight clients reveal to the server their public IP and the fact that they use Bitcoin, it is not straightforward for an adversarial server to map the IP to any specific Bitcoin address or transaction. It would be possible to do so by running Sybil nodes in the Bitcoin network itself [18], [16], [17], but such a threat is orthogonal to our protocol.

## 8. Implementation and Evaluation

We implemented our gossip-based protocol using the Python-Flask web framework [12]. The client side uses the Python Requests library that enables it to send custom HTTP request to servers with modified HTTP headers. We use Flask’s default web server to run the web application that supports our gossip-based protocol. At the server, block headers are buffered in its memory for faster access – however, we leave performance optimization as future work. In order to send the block headers which are stored as bytes, we use Base64 encoding to convert the bytes to strings before appending them to the HTTP header.

### Evaluation

We have built a custom testbed on Amazon AWS and then used it to evaluate our gossip-layer implementation. We conducted a series of experiments, picking a pair of virtual machine instances (t2.micro) running Linux Ubuntu 18.04 in two different cities across different continents, such that one acts as a web server and the other as a client.

To evaluate the latency inflation introduced by gossip messages, we measured the time for a HTTP request-response to complete in two different scenarios, case 1) a

		Servers			
		OH	SG	FR	SY
Clients	OH		0.15% (1.13ms)	0.12% (0.49ms)	0.12% (0.86ms)
	SG	0.11% (0.96ms)		0.11% (0.69ms)	0.04% (0.26ms)
	FR	0.28% (1.06ms)	0.05% (0.29ms)		0.06% (0.65ms)
	SY	0.09% (0.72ms)	0.23% (1.66ms)	0.11% (1.22ms)	

Table 8: The average percentage latency inflation with our enhancement when 72 block headers (12 hrs) are transferred.

normal HTTP request-response, case 2) A HTTP request-response with an additional payloads of 72 block headers (12 hrs) in the HTTP header. The time taken for each case was measured and repeated for 100 such HTTP request-response. The difference in time between the two cases is the introduced latency measured. The experiment was redone across different cities. The cities chosen are Ohio (OH), Singapore (SG), Frankfurt (FR), and Sydney (SY). Table 8 presents the average latency overhead while the client gossip 72 (12 hrs) of its block headers. The row and column are the locations of the client and the server respectively. The results show that the average latency inflation is just 0.12% which is negligible.

## 9. Conclusions

In this work, we have presented two lightweight protocols for the detection of eclipse attacks on Bitcoin clients. Our schemes either use block timestamps, or existing web servers to create an out-of-Bitcoin gossiping network basing on natural Internet traffic. We do not require any changes to the Bitcoin protocol or its network. Moreover, we demonstrate the effectiveness of our protocol by conducting a series of simulations using real Internet client-server communication traces and show that it is very efficient. We implemented the scheme by extending a web application to gossip block headers in its HTTP(S) header. We proposed a method for compressing Bitcoin subchains and evaluated our implementation with multiple experiments. Our analysis and evaluation indicate that the protocol provides multiple benefits, while introducing low overheads and a significantly improved detection time. Although our system was designed for Bitcoin, it can be directly applicable to Bitcoin forks and similar strongest-chain proof-of-work blockchains. Furthermore, we envision that the protocol can be extended to other classes of blockchain systems, like proof-of-stake schemes or permissioned blockchains, however we leave this as future work.

## References

- [1] Bitcoinj security model. <https://bitcoinj.github.io/security-model>, 2018 (accessed Jan 4, 2019).
- [2] Rfc 894. <https://tools.ietf.org/html/rfc894>, (accessed April 28th, 2019).
- [3] Opentimestamp. <https://opentimestamps.org/>, (accessed April 30th, 2019).

- [4] TUN/TAP virtual network interface. <https://www.kernel.org/doc/Documentation/networking/tuntap.txt>, (accessed Feb 06, 2019).
- [5] Bitcoinj checkpoint. <https://bitcoinj.github.io/speeding-up-chain-sync#checkpointing>, (accessed Feb 13, 2019).
- [6] Electrum SPV client checkpoint. <https://electrumx.readthedocs.io/en/latest/protocol-basics.html>, (accessed Feb 13, 2019).
- [7] Bitcoin transaction - Bitcoin Wiki. <https://en.bitcoin.it/wiki/Transaction>, (accessed Jan 19, 2019).
- [8] Protocol documentation: Block headers - Bitcoin Wiki. [https://en.bitcoin.it/wiki/Protocol\\_documentation#Block\\_Headers](https://en.bitcoin.it/wiki/Protocol_documentation#Block_Headers), (accessed Jan 19, 2019).
- [9] DNS bootstrap servers: Bitcoinstats. <http://bitcoinstats.com/network/dns-servers/>, (accessed Jan 25, 2019).
- [10] Bitcoin developer reference. <https://btcoinformation.org/en/developer-reference#target-nbits>, (accessed May 15, 2019).
- [11] How many confirmations is enough. [https://en.bitcoin.it/wiki/Confirmation#How\\_Many\\_Confirmations\\_Is\\_Enough](https://en.bitcoin.it/wiki/Confirmation#How_Many_Confirmations_Is_Enough), (accessed May 15, 2019).
- [12] Flask Web Framework. <https://github.com/pallets/flask>, (accessed Nov 9, 2019).
- [13] M. Al-Bassam, A. Sonnino, and V. Buterin. Fraud proofs: Maximising light client security and scaling blockchains with dishonest majorities. *arXiv preprint arXiv:1809.09044*, 2018.
- [14] M. Apostolaki, G. Marti, J. Müller, and L. Vanbever. SABRE: Protecting Bitcoin against routing attacks. *arXiv preprint arXiv:1808.06254*, 2018.
- [15] M. Apostolaki, A. Zohar, and L. Vanbever. Hijacking Bitcoin: Routing attacks on cryptocurrencies. In *Security and Privacy (SP), 2017 IEEE Symposium on*, pages 375–392. IEEE, 2017.
- [16] A. Biryukov, D. Khovratovich, and I. Pustogarov. Deanonymisation of clients in bitcoin p2p network. In *Proceedings of the 2014 ACM SIGSAC Conference on Computer and Communications Security*, pages 15–29. ACM, 2014.
- [17] A. Biryukov and S. Tikhomirov. Security and privacy of mobile wallet users in bitcoin, dash, monero, and zcash. *Pervasive and Mobile Computing*, page 101030, 2019.
- [18] G. Caffyn. Chainalysis ceo denies sybil attack on bitcoin network. <https://www.coindesk.com/chainalysis-ceo-denies-launching-sybil-attack-on-bitcoin-network>, 2015.
- [19] L. Chuat, P. Szalachowski, A. Perrig, B. Laurie, and E. Messeri. Efficient gossip protocols for verifying the consistency of certificate logs. In *Communications and Network Security (CNS), 2015 IEEE Conference on*, pages 415–423. IEEE, 2015.
- [20] C. Decker and R. Wattenhofer. Information propagation in the Bitcoin network. In *IEEE P2P 2013 Proceedings*, pages 1–10. IEEE, 2013.
- [21] C. Decker and R. Wattenhofer. A fast and scalable payment network with Bitcoin duplex micropayment channels. In *Symposium on Self-Stabilizing Systems*, pages 3–18. Springer, 2015.
- [22] S. N. . B. C. Developers. Bitcoin github repository. <https://github.com/bitcoin/bitcoin/blob/master/src/chainparams.cpp>, (accessed Jan 15, 2019).
- [23] A. Dunkels. Design and implementation of the lwIP TCP/IP stack. *Swedish Institute of Computer Science*, 2:77, 2001.
- [24] P. Ekparinya, V. Gramoli, and G. Jourjon. Impact of man-in-the-middle attacks on Ethereum. In *2018 IEEE 37th Symposium on Reliable Distributed Systems (SRDS)*, pages 11–20. IEEE, 2018.
- [25] A. Gervais, G. O. Karame, K. Wüst, V. Glykantzis, H. Ritzdorf, and S. Capkun. On the security and performance of proof of work blockchains. In *Proceedings of the 2016 ACM SIGSAC Conference on Computer and Communications Security*, pages 3–16. ACM, 2016.
- [26] A. Gervais, H. Ritzdorf, G. O. Karame, and S. Capkun. Tampering with the delivery of blocks and transactions in Bitcoin. In *Proceedings of the 22nd ACM SIGSAC Conference on Computer and Communications Security*, pages 692–705. ACM, 2015.
- [27] E. Heilman and A. Kendler. Eclipse attacks on Bitcoin’s peer-to-peer network: Video presentation. <https://www.usenix.org/node/190891>, (accessed Jan 20, 2019).
- [28] E. Heilman, A. Kendler, A. Zohar, and S. Goldberg. Eclipse attacks on Bitcoin’s peer-to-peer network. In *USENIX Security Symposium*, pages 129–144, 2015.
- [29] A. Kiayias, A. Miller, and D. Zindros. Non-interactive proofs of proof-of-work. Technical report, Cryptology ePrint Archive, Report 2017/963, 2017. Accessed: 2017-10-03, 2017.
- [30] B. Laurie, A. Langley, and E. Kasper. Certificate Transparency. RFC 6962, 2013.
- [31] A. F. Loe and E. A. Quaglia. You shall not join: A measurement study of cryptocurrency peer-to-peer bootstrapping techniques. In *Proceedings of the 2019 ACM SIGSAC Conference on Computer and Communications Security*, pages 2231–2247. ACM, 2019.
- [32] L. Luu, B. Buenz, and M. Zamani. Flyclient super light client for cryptocurrencies. Technical report, accessed 2018-04-17. Available: "https://eprint.iacr.org/2019/226.pdf".
- [33] Y. Marcus, E. Heilman, and S. Goldberg. Low-resource eclipse attacks on Ethereum’s peer-to-peer network. *IACR Cryptology ePrint Archive*, 2018:236, 2018.
- [34] S. Nakamoto. Bitcoin: A peer-to-peer electronic cash system. 2008.
- [35] K. Nayak, S. Kumar, A. Miller, and E. Shi. Stubborn mining: Generalizing selfish mining and combining with an eclipse attack. In *Security and Privacy (EuroS&P), 2016 IEEE European Symposium on*, pages 305–320. IEEE, 2016.
- [36] L. Nordberg, D. Gillmor, and T. Ritter. Gossiping in CT. *Internet-Draft draft-linus-trans-gossip-ct-04*, 2017.
- [37] S. Son and V. Shmatikov. The hitchhiker’s guide to DNS cache poisoning. In S. Jajodia and J. Zhou, editors, *Security and Privacy in Communication Networks*, pages 466–483, Berlin, Heidelberg, 2010. Springer Berlin Heidelberg.
- [38] P. Szalachowski. (short paper) Towards more reliable Bitcoin timestamps. *IEEE CVCBT*, 2018.
- [39] A. Tomescu and S. Devadas. Catena: Efficient non-equivocation via Bitcoin. In *2017 IEEE Symposium on Security and Privacy (SP)*, pages 393–409. IEEE, 2017.
- [40] M. Tran, I. Choi, G. J. Moon, A. V. Vu, and M. S. Kang. A Stealthier Partitioning Attack against Bitcoin Peer-to-Peer Network. In *To appear in Proceedings of IEEE Symposium on Security and Privacy (IEEE S&P)*, 2020.
- [41] U. W. Chohan. The double spending problem and cryptocurrencies. *SSRN Electronic Journal*, 01 2017.
- [42] W. Wang, D. T. Hoang, Z. Xiong, D. Niyato, P. Wang, P. Hu, and Y. Wen. A survey on consensus mechanisms and mining management in blockchain networks (figure 3). *arXiv preprint arXiv:1805.02707*, 2018.
- [43] K. Wüst and A. Gervais. Ethereum eclipse attacks. Technical report, ETH Zurich, 2016.

## Appendix A. TCP Gossip Layer

Another design choice of our architecture is implement the message exchange of our protocol as an extension of the transport layer, more specifically the TCP protocol. TCP is the de facto standard transport protocol of the Internet, ubiquitously used and implemented by a large number of existing protocols, devices, and operating systems. Therefore, any system running a modified TCP stack with the ability to store and process gossip messages is able to use the proposed protocol. Another advantage of using TCP as a gossip layer is its requires no changes to existing applications unlike our present implementation with HTTP. For these reasons, the adoption of our protocol could be accelerated and our protocol could perform better

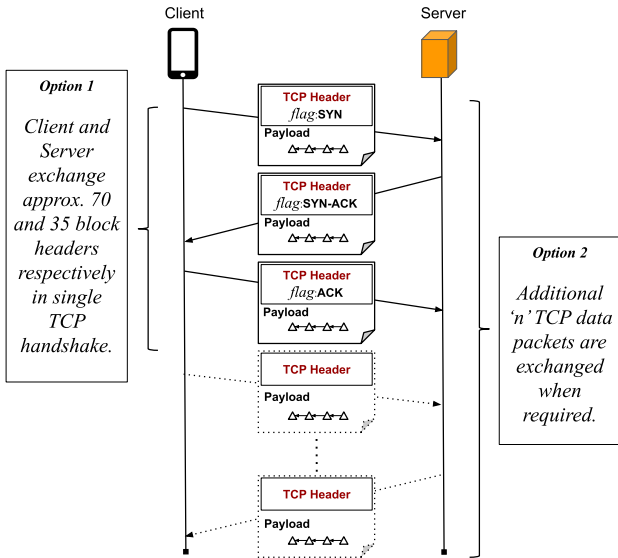


Figure 8: Our protocol implemented by extending a 3-way-TCP handshake between a client and server. Option 1 is used when all data requests fits in a 3-Way-Handshake. Option 2 is used to exchange additional data packets.

in eclipse attack detection (as the protocol can be executed seamlessly between a large number of clients and servers).

More concretely, to minimize the latency inflation caused by sending Bitcoin headers, we implement our message exchange as data piggybacked on the TCP handshake. We leverage the fact that the TCP handshake consists of three messages that do not carry data.<sup>7</sup> Hence, we minimize introduced latency by exchanging block headers via TCP handshake messages (sent anyway while establishing a TCP connection).

As seen in Figure 8, a client initiates a TCP handshake with a server and two options are supported. In option 1, the requested block headers are fully exchanged within a 3-way TCP handshake. However, limitations to the number of block headers that can fit into a TCP packet implies that further communication may be needed to send any outstanding block headers. In this case, our protocol introduces latency inflation and this scenario is illustrated as option 2. The client and server are seen to have additional block headers delivered in the data exchange that follows. Usually, each TCP packet is limited to 1500 bytes.<sup>8</sup> This approximately corresponds to 35 reduced-size block headers (each 40 bytes) that can be communicated in a single packet of the TCP handshake. Therefore, with a TCP handshake only (i.e., SYN, SYN-ACK, and ACK), the server can receive up to 70 headers from the client and the client can receive up to 35 headers from the server, which is near to 12 and 6 hours of block header data respectively (with an average 10 minute inter-block delay).

7. Carrying data on TCP handshake packets is allowed by the TCP specification, although such data is not passed to applications. It does not influence our protocol as it is implemented at the TCP (not application) layer.

8. 1500 bytes is the standard Internet MTU [2].

## Implementation

To implement our protocol we extended an existing TCP stack. The gossip layer is implemented on Lightweight IP (LwIP) [23], a state-of-the-art userspace TCP implementation used in production by many systems. With our implementation, the server and client run a modified TCP stack to communicate on the network through a TAP/TUN interface [4]. The TCP three-way handshake is initiated by calling `tcp_connect()` which in turn calls `tcp_enqueue_flags()`, to build the packets with the required TCP flags. We modified this API to allow piggybacking our gossiping messages on TCP handshake packets. The following code snippet gives an overview of the modified `tcp_enqueue_flags()` function that caters for gossip messaging.

```
tcp_enqueue_flags(pcb, flags,
                  gossipMsg) {
    gossip_len = sizeof(gossipMsg)
    packet = pbuf_alloc(PBUF_TRANSPORT,
                       optlen + gossip_len,
                       PBUF_RAM)
    TCP_DATA_COPY2(packet->payload +
                   optlen, gossipMsg)
    seg = tcp_create_segment(pcb,
                             packet, flags,
                             pcb->snd_lbb,
                             optflags))
}
```

The `tcp_enqueue_flags()` function takes three arguments, namely: protocol control block (`pcb`), TCP flags, and a gossip message of our protocol. The `pbuf_alloc()` function is responsible for memory allocation and in our case we have to adjust the parameters of this functions such that an additional memory for the gossip message is allocated. The `TCP_DATA_COPY2()` function is a variant of a memory copy function used to copy the gossip message onto the packet. The `tcp_create_segment()` function creates a TCP segment, with the required gossip message. At the receiving end, TCP segments are handled by the `tcp_input()` function.

```
tcp_input(tcp_segment) {
    removeHeaders(tcp_segment->payload)
    MEMCPY(buffer, tcp_segment->payload,
           tcp_segment->length)
}
```

With this call, the packet header in `tcp_segment->payload` is removed and the received gossip message (block headers) is left. It is copied to the `buffer` for further processing of our protocol. We implemented a simple file transfer (client-server) application using our modified stack.

## Evaluation

The setup is similar to Section 8,

In this case also, we measured the time for a TCP connection establishment in two different scenarios, case 1) A normal TCP handshake, case 2) A TCP handshake with an additional payload of 1440 bytes (including 35 block

Clients	Servers			
	OH	SG	FR	SY
OH		2.26% (2.22ms)	2.39% (2.33ms)	1.22% (2.35ms)
SG	1.09% (2.39ms)		1.47% (2.52ms)	1.32% (2.31ms)
FR	2.36% (2.30ms)	1.28% (2.22ms)		0
SY	1.23% (2.37ms)	1.32% (2.22ms)	0	

Table 9: The average percentage latency inflation with our enhancement.

headers). The time taken for each case was measured and repeated for 100 such TCP handshakes. The difference in time between the two cases is the introduced latency measured. The experiment was redone across different cities. Table 9 presents the average latency overhead. On an average, the overhead is seen to be close to 1.59%. For handshakes between Frankfurt and Sydney, no overhead was recorded and may be attributed to high network latency.

## Appendix B. HTTP body Gossip-Layer

In this section we present the results for evaluation of our gossiping using HTTP body. Unlike sending data in HTTP headers of request-response message. Here, we provide an implementation based on sending the block headers as file chunks in HTTP body with 72 (12 hrs), 144 (24 hrs), 1008 (7 days) and 2016 (14 days) block headers. The results are presented in tables Table 12, Table 13, Table 10, and Table 11 respectively. The experimental setup and evaluation methodology is exactly same as in Section 8.

Clients	Servers			
	OH	SG	FR	SY
OH		149.56% (1338.74ms)	148.77% (1162.44ms)	152.82% (579.62ms)
SG	149.94% (1341.85ms)		143.03% (982.34ms)	153.66% (1106.01ms)
FR	149.09% (581.06s)	163.08% (1094.42ms)		152.02% (1740.01ms)
SY	150.14% (1142.51ms)	176.30% (1269.78ms)	150.78% (1724.61ms)	

Table 10: The average percentage latency inflation with our enhancement when 2016 block headers (14 days) are transferred.

As we can see the latency inflation is almost on an average 100% for block headers generated over a week and increases by 50-60% for two weeks. In case of 12 hrs i.e. 72 block headers the average latency inflation is 0.08% and increase with 24 hrs block headers. The results indicate that the inflation remains negligible if the users come online for at least once in a day which is not unrealistic with the present day Internet users.

In Figure 9 and Figure 10 show the average latency for HTTP request-response for clients with our enhance while they are placed at OH, SG, FR and SY. The results prove that the latency only grows linearly with increase in number of block headers.

Clients	Servers			
	OH	SG	FR	SY
OH		99.63% (891.71ms)	99.32% (386.94ms)	128.35% (976.29ms)
SG	99.58% (0.19ms)		99.02% (0.53ms)	100.68% (1.46ms)
FR	99.31% (387.01ms)	100.72% (675.87ms)		99.87% (1143.12ms)
SY	99.57% (757.62ms)	100.38% (722.98ms)	99.76% (1141.07ms)	

Table 11: The average percentage latency inflation with our enhancement when 1008 block headers (7 days) are transferred.

Clients	Servers			
	OH	SG	FR	SY
OH		0.04% (0.27ms)	0.21% (0.79ms)	0.03% (0.21ms)
SG	0.10% (0.89ms)		0.04% (0.41ms)	0.06% (0.41ms)
FR	0.20% (0.80ms)	0.02% (0.11ms)		0.04% (0.42ms)
SY	0.01% (0.05ms)	0.13% (0.9ms)	0.07% (0.69ms)	

Table 12: The average percentage latency inflation with our enhancement when 72 block headers (12 hrs) are transferred in HTTP body.

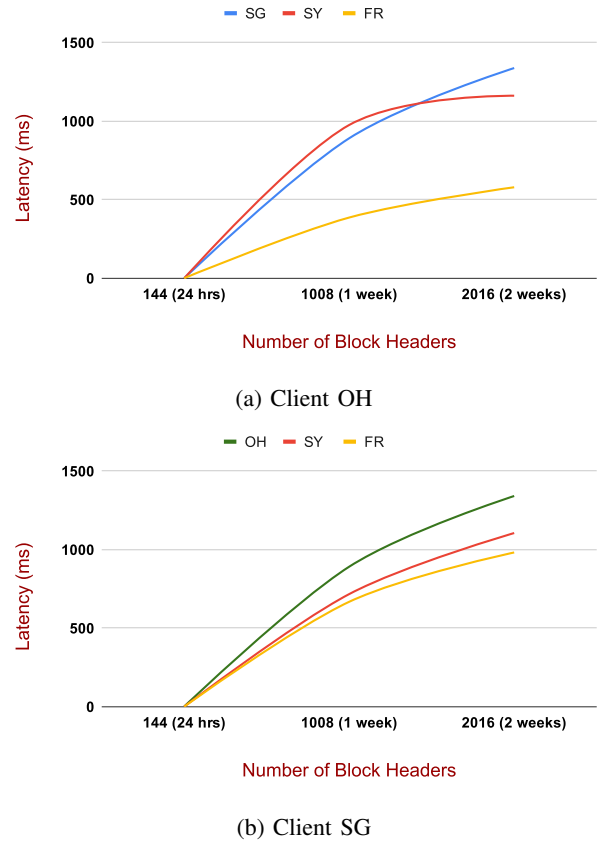
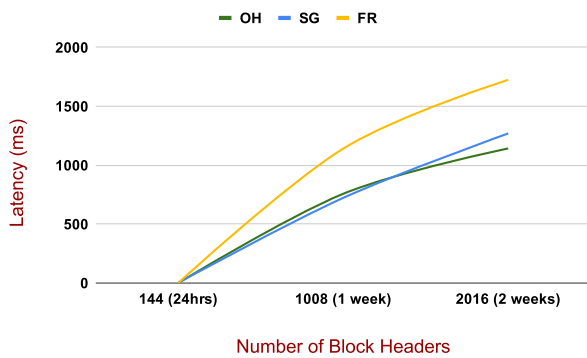


Figure 9: (a) The average latency when client is at OH and gossips with server at SG, SY and FR, (b) The average latency when client is at SG and gossips with server at OH, SY and FR.

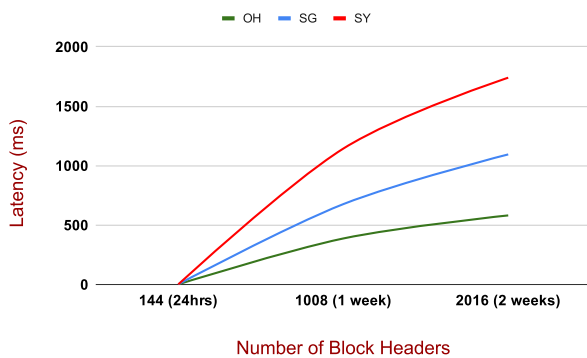


Clients	Servers			
	OH	SG	FR	SY
OH		0.09% (0.78ms)	0.25% (1.01ms)	0.07% (0.48ms)
SG	0.21% (1.92ms)		0.16% (1.10ms)	0.13% (0.91ms)
FR	0.28% (1.08ms)	0.28% (1.85ms)		0.07% (0.7ms)
SY	0.04% (0.30ms)	0.32% (2.29ms)	0.08% (0.84ms)	

Table 13: The average percentage latency inflation with our enhancement when 144 block headers (24 hrs) are transferred.



(a) Client SY



(b) Client FR

Figure 10: (a) The average latency when client is placed at SY and gossip with server at OH, SG and FR, (b) The average latency when client is placed at SG and gossip with server at OH, SY and FR.